DOI: 10.30511/pcdp.2025.2055897.1020 - ISSN: 3060-8376 - Vol 2(2), 2025

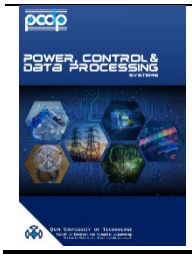

POWER, CONTROL AND DATA PROCESSING SYSTEMS

Available Online at: https://pcdp.qut.ac.ir/

Finite Time Power Regulation of BDFIG Using Adaptive Nonlinear Method

ARTICLE INFO

Article Type
Original Research

Authors
Mohsen Ehsani[1]
Vahid Behnamgol[1*]
Ashknaz Oraee[1]
Roohollah Barzamini[2]
Behnaz Sohani[3]

[1] Damavand Branch, Islamic Azad University, Tehran, Iran. (m.ehsani@damavandiau.ac.ir); (vahid_behnamgol@damavandiau.ac.ir); (ashknaz.oraee@gmail.com)
[2] Department of Electrical Engineering, Central Tehran Branch, Islamic Azad University, Tehran, Iran (r.barzamini.eng@iauctb.ac.ir)
[3] Wolfson School of Mechanical, Electrical & Manufacturing Engineering, Loughborough University, Loughborough, Leicestershire, LE11 3TU, UK (b.sohani@lboro.ac.uk)

**** Correspondence***
vahid_behnamgol@damavandiau.ac.ir

Article History
Received: March 13, 2025
Accepted: April 03, 2025
ePublished: June 01, 2025

ABSTRACT

This paper presents a novel finite-time adaptive dynamic sliding mode controller (SMC) for regulating the power of a brushless double-fed induction generator (BDFIG). Wind turbines equipped with BDFIGs present unique challenges due to the system's nonlinear dynamics, external disturbances, and inherent uncertainties. To address these issues, SMC is employed for its robustness and effectiveness in uncertain environments. The proposed controller integrates a dynamic SMC, ensuring a smooth control signal and mitigating the chattering effect commonly associated with conventional SMCs. A key innovation of this work is the development of an adaptive gain mechanism that eliminates the need for prior knowledge of uncertainty bounds. This adaptive gain dynamically converges to the upper bound of uncertainties, enhancing the system's adaptability and robustness. Using the Lyapunov stability theorem, finite-time convergence is rigorously proven, ensuring that the sliding variable reaches zero within a finite time, and the adaptive gain aligns with the uncertainty bound.

Keywords: BDFIG, Dynamic Control, Adaptive SMC, Finite-time Stability.

1 Introduction

Growing concerns about climate change in recent years have driven extensive efforts to develop clean and cost-effective power generation methods. This has sparked significant interest in renewable energy systems, which have advanced remarkably due to improvements in converter technologies and control strategies. Among these, the brushless double-fed induction generator (BDFIG) has attracted considerable attention for its exceptional performance under variable wind speed conditions [1].

The BDFIG represents a promising alternative to the conventional doubly fed induction generator (DFIG) for wind turbine applications, offering enhanced reliability while reducing capital and maintenance costs. It maintains the cost-efficiency of the traditional DFIG system, as it only requires a fractionally rated converter and eliminates the need for permanent magnet materials.

The elimination of brushes and rotor contact in the BDFIG removes a common failure point, making it especially suitable for offshore wind applications. Additionally, as a medium-speed machine, the BDFIG enables the use of simplified gearboxes with one or two stages, further enhancing its efficiency [2].

The BDFIG features two stator windings: the Power Winding (PW), which connects directly to the power grid, and the Control Winding (CW), which interfaces with a bidirectional power converter.

Despite the development of several control strategies for BDFIGs, their complex coupled models present significant challenges in designing robust, high-performance controllers. Nonlinear controllers have thus been explored to improve system robustness [3, 4].

Sliding Mode Control (SMC) has been employed in BDFIG systems to address control challenges. For example, an integrated SMC in [4] was used to eliminate speed errors and suppress disturbances in brushless doubly fed machines. Similarly, SMC achieved smooth grid synchronization and flexible power adjustment in [5]. In [6], sliding mode control was applied for both grid-connected and islanded operations of a brushless DFIG wind turbine. Predictive SMC, coupled with Particle Swarm Optimization (PSO) for tuning, was used in [7] to regulate active and reactive power, while additional SMC strategies for BDFIGs were explored in [8].

However, first-order sliding mode control suffers from a phenomenon called chattering, which results from the use of a sign function in the control signal [9]. Chattering is an undesirable effect that complicates practical implementation. To mitigate this issue, various approaches have been proposed. One simple solution involves replacing the discontinuous control function with a continuous approximation within a boundary layer. Alternatively, high-order SMC (HOSMC) has been introduced to achieve smoother control signals. For instance, second-order SMC (SOSMC) techniques, such as the super-twisting algorithm, have been applied to brushless DFIG systems [1, 10, 11]. However, HOSMC methods often require complex stability proofs and do not easily determine convergence time for the sliding variable.

Dynamic Sliding Mode Control (DSMC) offers another solution to address chattering. DSMC, ensures the smoothness of the resulting control signal after integration [12–14]. DSMC provides better performance and stability, particularly in systems with uncertainties [15]. Variants such as dynamic integral sliding mode control [16] and fractional-order DSMC [17, 18] have also been developed to reduce chattering. Improvements, including faster reaching phases [19] and robustness under mismatched uncertainties [20], have further enhanced DSMC methods. Observer-based DSMC approaches have also been proposed, but these still exhibit chattering effects due to Proportional-Integral (PI) sliding surfaces [21].

Another challenge in SMC is the requirement for an upper bound on system uncertainties. Adaptive Sliding Mode Control (ASMC) has been developed to address this issue by introducing adaptive switching gains that adjust to unknown uncertainty bounds [22–26]. However, while ASMC improves robustness, it often fails to ensure finite-time stability of the sliding variable and adaptive gain, which is critical for tracking applications. Additionally, overestimated gains can result in larger control magnitudes and increased chattering [23, 26].

This study aims to design a nonlinear control strategy that ensures finite-time regulation of powers in a BDFIG, while generating smooth signals without the need for prior knowledge of uncertainty bounds. To this end, an Adaptive Dynamic SMC (ADSMC) strategy is proposed. Unlike conventional adaptive SMC, the proposed method ensures finite-time convergence of both the sliding variable and the adaptive gain. By integrating dynamic sliding mode control, the system achieves smooth control performance even under uncertainty.

The structure of this paper is as follows: Section 2 presents the mathematical model of the BDFIG. Section 3 introduces the finite-time adaptive dynamic sliding mode control theory, while Section 4 discusses its application for controlling the brushless DFIG. Simulation results are provided in Section 5. Finally, conclusions are presented in Section 6.

2 BDFIG Mathematical Model

The equations for the BDFIG are presented in the d-q coordinate system, as described in [1] and [27]. The angular velocity of the stator power winding is denoted by ω_{sp}, and the rotor angular velocity is given by:

$$\omega_r = \frac{\omega_{sc} \pm \omega_{sp}}{P_c + P_p} \tag{1}$$

The flux, voltage, and current relationships in the stator and rotor for the power and control sections are as follows:

$$v_{sp} = R_{sp} I_{sp} + \frac{d}{dt}\Phi_{sp} + j\omega_{sp}\Phi_{sp}\theta$$

$$v_{sc} = R_{sc} I_{sc} + \frac{d}{dt}\Phi_{sc} + j\left(\omega_{sp} - \left(p_p + p_c\right)\omega_r\right)\Phi_{sc}$$

$$v_r = R_r I_r + \frac{d}{dt}\Phi_r + j(\omega_{sp} - p_p\omega_r)\Phi_r \quad (2)$$

The flux relationship can be introduced as follows:

$$\Phi_{sp} = L_{sp}I_{sp} + M_p I_r$$
$$\Phi_{sc} = L_{sc}I_{sc} + M_c I_r$$
$$\Phi_r = L_r I_r + M_c I_{sc} + M_p I_{sp} \quad (3)$$

The electromagnetic torque is given by:

$$T_{em} = \frac{3}{2}P_p M_p\left(I_{sp}^q I_r^d - I_{sp}^d I_r^q\right) - \frac{3}{2}P_c M_c\left(I_{sc}^q I_r^d - I_{sc}^d I_r^q\right) \quad (4)$$

The stator powers expressions are as follows:

$$P_{sp} = \frac{3}{2}\left(v_{sp}^d I_{sp}^d + v_{sp}^q I_{sp}^q\right)$$
$$Q_{sp} = \frac{3}{2}\left(v_{sp}^q I_{sp}^d + v_{sp}^d I_{sp}^d\right) \quad (5)$$

From equation (3), the following results can be obtained:

$$I_{sp} = \frac{\Phi_{sp} - M_p I_r^d}{L_{sp}}$$
$$I_r = \frac{\Phi_r - M_p I_{sp} - M_c I_{sc}}{L_r} \quad (6)$$

It can be concluded from equations (3) and (6):

$$I_{sp} = \frac{L_r}{L_{sp}L_r - M_p^2}\Phi_{sp} + \frac{M_p}{L_{sp}L_r - M_p^2}\Phi_r + \frac{M_c M_p}{L_{sp}L_r - M_p^2}I_{sc} \quad (7)$$

Substitution of (6) into equations (3) and (4) gives:

$$P_{sp} = \frac{3}{2}V_{sp}\left(\lambda_5\Phi_{sp}^q - \lambda_4\Phi_r^q + \lambda_3 I_{sc}^q\right)$$
$$Q_{sp} = \frac{3}{2}V_{sp}\left(\lambda_5\Phi_{sp}^d - \lambda_4\Phi_r^d + \lambda_3 I_{sc}^d\right) \quad (8)$$

Where:

$$\lambda_1 = \frac{L_{sp}M_c}{L_r L_{sp} - M_p^2}, \lambda_2 = L_{sc} - \frac{L_{sp}M_c^2}{L_r L_{sp} - M_p^2},$$
$$\lambda_3 = \frac{M_c M_p}{L_r L_{sp} - M_p^2}, \lambda_4 = \frac{M_p}{L_r L_{sp} - M_p^2},$$
$$\lambda_5 = \frac{L_r}{L_r L_{sp} - M_p^2} \quad (9)$$

Lastly, the dynamic interaction between the control winding current and the d–q axis voltages can be expressed as:

$$V_{sc}^d = R_{sc}I_{sc}^d\left(\frac{d}{dt}(\lambda_1\Phi_r^d + \lambda_2 I_{sc}^d) - \omega_{sc}(\lambda_1\Phi_r^q + \lambda_2 I_{sc}^q - \lambda_3\Phi_{sp}^q)\right)$$
$$V_{sc}^q = R_{sc}I_{sc}^q\left(\frac{d}{dt}(\lambda_1\Phi_r^q + \lambda_2 I_{sc}^q) + \omega_{sc}(\lambda_1\Phi_r^d + \lambda_2 I_{sc}^d - \lambda_3\Phi_{sp}^d)\right) \quad (10)$$

3 Main Results

3.1 Sliding Mode Control

Consider a nonlinear system as:

$$\dot{x} = f(x) + g(x)u + d(t) \quad (11)$$

where x is a vector of state variables, u is a control input and $f(x)$ is a nonlinear function vector-field.

Assuming the sliding variable is defined such that its zeroing ensures desirable behavior for system (11), the relative degree of the sliding variable with respect to the control input is one, and the internal dynamics of system (11) remain stable. Consequently, the input–output dynamics can be described as:

$$\dot{s} = \frac{\partial s}{\partial t} + \frac{\partial s}{\partial x}f(x) + \frac{\partial s}{\partial t}g(x)u = a(x,t) + b(x,t)u \quad (12)$$

The function $b(x,t)$ is known, and the function $a(x,t)$ is expressed as $a(x,t) = \bar{a}(x,t) + d$where $\bar{a}(x,t)$ and d are the known and unknown parts of $a(x,t)$, respectively. Additionally, it is assumed that the uncertainty is constrained within the bound $|d| \le L_d$. The objective is to develop a control input that effectively addresses uncertainties, ensuring that the sliding variable converges to zero.

Standard first-order SMC ensures the finite-time convergence of the sliding variable to zero [28]. In traditional SMC, the controller is defined as follows:

$$u = \frac{1}{b(x,t)}[-\bar{a}(x,t) - ksign(s)] \quad (13)$$

where $k = \eta + L_d$ is the switching gain. By applying the controller from equation (13) to the sliding variable dynamics in equation (12), the sliding variable s remains the only variable. To verify its stability, the candidate Lyapunov function is selected as $V = \frac{1}{2}s^2$. To ensure finite-time stabilization, $\dot{V} = s\dot{s} \le -\eta|s|$condition must be satisfied, where η is a strictly positive constant, leading to the reaching time $t_r \le \frac{|s(0)|}{\eta}$ [29].

In the dynamic sliding mode method [17], the new sliding variable is introduced as $\sigma = \dot{s} + \lambda s$ where $\lambda > 0$. When $\sigma = 0$, $\dot{s} + \lambda s = 0$ is asymptotically stable, $e \to 0$ and $\dot{e} \to 0$. Therefore, we have:

$$\dot{\sigma} = \alpha(x,u) + \beta\dot{u} + D$$
$$\alpha = \left(\dot{\bar{a}}(x,t) + \lambda\bar{a}(x,t) + \left(\dot{b}(x,t) + \lambda b(x,t)\right)u\right)$$
$$\beta = b(x,t),\ D = \left(\dot{d} + \lambda d\right) \quad (14)$$

The dynamic control input is selected as:

$$\dot{u} = \frac{1}{\beta}(-\alpha(x,u) - k\,sgn(\sigma)) \quad (15)$$

where $k = \eta + L_{\dot{d}} + \lambda L_d$ is the reaching term. Given that equation (14) in the dynamic system has a relative order of one and contains only the σvariable, the candidate Lyapunov function $V = \frac{1}{2}\sigma^2$ is selected to verify stability. By selecting this candidate Lyapunov function, condition $\dot{V} = \sigma\dot{\sigma} \le -\eta|\sigma|$ must be satisfied to achieve finite-time stabilization of the sliding variable, where η is a strictly positive constant, which implies $t_r \le \frac{|\sigma(0)|}{\eta}$.

Determining the switching gain for the control inputs in (13) and (15) requires knowledge of the uncertainty term upper bound. If this bound is unknown, the adaptive SMC can be applied. This approach, allows for adaptive adjustment of the switching term [26]. In this method, the controller is defined in (16) for sliding variable dynamics (12), eliminating the need for the uncertainty upper bound.

$$\begin{cases} u = \frac{1}{b(x,t)}\left(-\bar{a}(x,t) - \hat{k}(t)sign(s)\right) \\ \dot{\hat{k}}(t) = k_0|s| \\ k_0 > 0 \end{cases} \quad (16)$$

The adaptive gain mechanism operates without requiring prior knowledge of the uncertainty upper bound. In adaptive SMC, the switching gain is dynamically adjusted based on real-time estimations of system uncertainties, rather than relying on a predefined upper bound. This dynamic adjustment enhances robustness by allowing the controller to adapt its gain to varying levels of uncertainty, ensuring system stability and finite-time convergence.

According to relation (16), the adaptive law continuously updates the gain based on variations in the sliding variable. When relation (16) is applied to the sliding variable dynamics, we obtain $\dot{s} = d - \hat{k}(t)sign(s)$. As demonstrated in Figure 1 with a simple example, the sliding variable is non-zero when uncertainty is present, and the adaptive gain converges to the uncertainty bound L_d, ensuring robust control performance. Once the adaptive gain reaches the uncertainty upper bound, the sliding variable reduces to zero. This process eliminates the need for conservative overestimation, which could otherwise result in excessive control efforts or chattering effects.

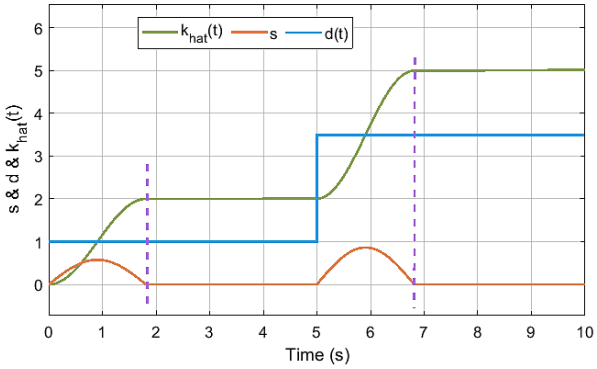

Fig. 1. Sliding variable, adaptive gain and uncertainty in the adaptive SMC

By applying the adaptive sliding mode control from equation (16) to the sliding variable dynamics in equation (14), the closed-loop system variables are $\sigma$and the estimation error $(\hat{k} - L_d)$. To verify the stability of these variables, the candidate Lyapunov function is selected as follows:

$$V = \frac{1}{2}s^2 + \frac{1}{2k_0}(\hat{k} - L_d)^2 \tag{17}$$

The derivative of the Lyapunov function can be expressed as follows:

$$\dot{V} = s\dot{s} + \frac{1}{k_0}(\hat{k} - L_d)\dot{\hat{k}} = + d(t)s - L_d|s| < 0 \tag{18}$$

Therefore, $s$and $\hat{k} - L_d$ are stable.

By using the control input in (16), the stability of the sliding variable is guaranteed, and the adaptive term also converges to the uncertainty upper bound [26]. It is worth noting that not accounting for the uncertainty upper bound in the proposed method results in a finite amount of time for the adaptive gain to reach the uncertainty bound.

3.2 Finite-time Adaptive Dynamic SMC

To ensure a smooth signal and maintain independence from the uncertainty bound, this study combines dynamic and adaptive SMC methods. Conventional adaptive sliding mode methods guarantee stability for both the sliding variable and the adaptive gain but fail to ensure finite-time convergence. This study addresses this limitation by combining a novel adaptive sliding mode approach with the dynamic sliding mode method and applying it to BDFIG control. In this case, the control input relationship in (15) is modified as follows:

$$\begin{cases} \dot{u} = \frac{1}{\beta}\left(-\alpha(x,u) - k_1|\sigma|^{\alpha}\hat{k}sign(\sigma) + u_s\right) \\ \dot{\hat{k}} = \frac{1}{\mu}(|\sigma| + k_1|\sigma|^{\alpha+1}) \\ \dot{u}_s = -|u_s|\sigma - \left(\hat{k}|\sigma| + q\right)sign(u_s) \end{cases} , \; 0 < \alpha < 1 \tag{19}$$

where k_1 and μ are positive constants, $\hat{k}$ is the estimation of the uncertainty bound, and u_s represents the auxiliary stabilizer control component.

Using the controller (19) in system (14), the closed-loop system will be in the following form:

$$\begin{cases} \dot{\sigma} = -k_1|\sigma|^{\alpha}\hat{k}sign(\sigma) + u_s + D \\ \dot{\hat{k}} = \frac{1}{\mu}(|\sigma| + k_1|\sigma|^{\alpha+1}) \\ \dot{u}_s = -|u_s|\sigma - \left(\hat{k}|\sigma| + q\right)sign(u_s) \end{cases} , \; 0 < \alpha < 1 \tag{20}$$

The closed-loop system variables are σ, the estimation error $(\hat{k} - L_d)$ and u_s. To verify the convergence of these variables, the candidate Lyapunov function is selected as follows:

$$V = \frac{1}{2}\sigma^2 + \frac{\mu}{2}\left(\hat{k} - L_d\right)^2 + |u_s| \tag{21}$$

The derivative of the Lyapunov function can be expressed as follows:

$$\begin{aligned} \dot{V} &= \sigma(-k\hat{k}|\sigma|^{\alpha}sign(\sigma) + u_s + d) \\ &\quad + (\hat{k} - L_d)(|\sigma| + k|\sigma|^{\alpha+1}) \\ &\quad + \frac{u_s}{|u_s|}(-|u_s|\sigma - \left(\hat{k}|\sigma| + q\right)sign(u_s)) \\ &= -k\hat{k}|\sigma|^{\alpha+1} + u_s\sigma + d\sigma + \hat{k}|\sigma| + \hat{k}k|\sigma|^{\alpha+1} \\ &\quad - L_d|\sigma| - L_dk|\sigma|^{\alpha+1} - u_s\sigma - \hat{k}|\sigma| - q \\ &\leq d\sigma - L_d|\sigma| - q \leq -q \end{aligned} \tag{22}$$

The condition (22) implies

$$\begin{aligned} &\int_{V(0)}^{0} dV \leq \int_{0}^{t} -\eta dt \\ &-V(0) \leq -\eta t \\ &t \leq \frac{V(0)}{\eta} \end{aligned} \tag{23}$$

Therefore condition (22) guarantees the stability of V in finite time (23) [23].

3.3 Finite-Time ADSMC for Brushless DFIGs

This section applies the proposed finite-time adaptive dynamic SMC theory to regulate powers of a BDFIG.
The relationships for the CW currents in the d-q coordinate system are expressed as follows:

$$\begin{cases} I_{sc}^{d} = \frac{Q_{sp}}{1.5V_{sp}^{q}\lambda_3} + \frac{\lambda_4}{\lambda_3}\,v_r^{d} - \frac{\lambda_5}{\lambda_3}\,v_{sp}^{d} \\ I_{sc}^{q} = \frac{P_{sp}}{1.5V_{sp}^{q}\lambda_3} + \frac{\lambda_4}{\lambda_3}\,v_r^{q} \end{cases} \quad (24)$$

Therefore, the desired currents based on the desired active and reactive powers can be calculated as:

$$\begin{cases} I_{sc}^{d\_ref} = \frac{Q_{sp}^{ref}}{1.5V_{sp}^{q}\lambda_3} + \frac{\lambda_4}{\lambda_3}\,v_r^{d} - \frac{\lambda_5}{\lambda_3}\,v_{sp}^{d} \\ I_{sc}^{q\_ref} = \frac{P_{sp}^{ref}}{1.5V_{sp}^{q}\lambda_3} + \frac{\lambda_4}{\lambda_3}\,v_r^{q} \end{cases} \quad (25)$$

Using sliding mode control theory, the sliding variables are defined as:

$$\begin{cases} S(P_{sp}) = \left(I_{sc}^{q} - I_{sc}^{q\_ref}\right) \\ S(Q_{sp}) = \left(I_{sc}^{d} - I_{sc}^{d\_ref}\right) \end{cases} \quad (26)$$

Then, we have:

$$\begin{cases} \dot{S}(P_{sp}) = \frac{V_{sc}^{q}}{\lambda_2} - \frac{R_{sc}}{\lambda_2} I_{sc}^{q} + \frac{\omega_{sc}}{\lambda_2}(\lambda_1 v_r^{d} + \lambda_2 I_{sc}^{d} - \lambda_3 v_{sp}^{d}) \\ \qquad - \frac{\lambda_1}{\lambda_2}\dot{v}_r^{q} - \dot{I}_{sc}^{q\_ref} = b_P u_P + d_P(t) \\ \dot{S}(Q_{sp}) = \frac{V_{sc}^{d}}{\lambda_2} - \frac{R_{sc}}{\lambda_2} I_{sc}^{d} + \frac{\omega_{sc}}{\lambda_2}(\lambda_1 v_r^{q} + \lambda_2 I_{sc}^{q}) \\ \qquad - \frac{\lambda_1}{\lambda_2}\dot{v}_r^{d} - \dot{I}_{sc}^{d\_ref} = b_Q u_Q + d_Q(t) \end{cases} \quad (27)$$

Where $b_P = \frac{1}{\lambda_2}$, $u_P = V_{sc}^{q}$, $b_Q = \frac{1}{\lambda_2}$, $u_Q = V_{sc}^{d}$, $d_P(t) = -\frac{R_{sc}}{\lambda_2} I_{sc}^{q} + \frac{\omega_{sc}}{\lambda_2}(\lambda_1 \Phi_r^{d} + \lambda_2 I_{sc}^{d} - \lambda_3 \Phi_{sp}^{d}) - \frac{\lambda_1}{\lambda_2}\dot{\Phi}_r^{q} - \dot{I}_{sc}^{q\_ref}$ and $d_Q(t) = -\frac{R_{sc}}{\lambda_2} I_{sc}^{d} + \frac{\omega_{sc}}{\lambda_2}(\lambda_1 \Phi_r^{q} + \lambda_2 I_{sc}^{q}) - \frac{\lambda_1}{\lambda_2}\dot{\Phi}_r^{d} - \dot{I}_{sc}^{d\_ref}$.
Based on the DSMC approach, the dynamic switching functions are obtained using:

$$\begin{aligned} \sigma(P_{SP}) &= \dot{S}(P_{sp}) + \lambda_P S(P_{sp}) \\ \sigma(Q_{SP}) &= \dot{S}(Q_{sp}) + \lambda_Q S(Q_{sp}) \end{aligned} \quad (28)$$

where $\lambda_P, \lambda_Q > 0$. The derivation of (28) is:

$$\begin{aligned} \dot{\sigma}(P_{SP}) &= \dot{b}_P u_P + b_P \dot{u}_P + \dot{d}_P(t) \\ &\quad + \lambda_P(b_P u_P + d_P(t)) = \beta_P \dot{u}_P + D_p \\ \dot{\sigma}(Q_{SP}) &= \dot{b}_Q u_Q + b_Q \dot{u}_Q + \dot{d}_Q(t) \\ &\quad + \lambda_Q\left(b_Q u_Q + d_Q(t)\right) = \beta_Q \dot{u}_Q + D_Q \end{aligned} \quad (29)$$

Where $\beta_P = b_P, D_p = \dot{b}_P u_P + \dot{d}_P(t) + \lambda_P(b_P u_P + d_P(t))$, $\beta_Q = b_Q$ and $D_Q = \dot{b}_Q u_Q + \dot{d}_Q(t) + \lambda_Q\left(b_Q u_Q + d_Q(t)\right)$. The finite-time adaptive dynamic SMC is expressed as:

$$\begin{cases} \dot{u}_p = \frac{1}{\beta_p}\left(-k_{1p}|\sigma_p|^{\alpha}\hat{k}_p sign(\sigma_p) + u_s\right) \\ \dot{\hat{k}}_p = \frac{1}{\mu}\left(|\sigma_p| + k_p|\sigma_p|^{\alpha+1}\right) \\ \dot{u}_s = -|u_s|\sigma_p - \left(\hat{k}_p|\sigma_p| + q_p\right)sign(u_s) \end{cases}, \; 0 < \alpha < 1$$

$$\begin{cases} \dot{u}_Q = \frac{1}{\beta_Q}\left(-k_{1Q}|\sigma_Q|^{\alpha}\hat{k}_Q sign(\sigma_Q) + u_s\right) \\ \dot{\hat{k}}_Q = \frac{1}{\mu}\left(|\sigma_Q| + k_Q|\sigma_Q|^{\alpha+1}\right) \\ \dot{u}_s = -|u_s|\sigma_Q - \left(\hat{k}_Q|\sigma_Q| + q_Q\right)sign(u_s) \end{cases}, \; 0 < \alpha < 1 \quad (30)$$

4 Simulation results

The proposed controller's performance was validated using MATLAB software and compared against the PID and SMC controllers. Table 1 provides the necessary gains used in the simulations. In the wind turbine management system, the controller operates for 2 seconds. Between 8 and 10 seconds, the control algorithm is disengaged due to a voltage dip, and the rotor current is monitored.

TABLE I. BDFIG PARAMETERS [27]

Parameter	Value
Frame size	D180
PW pole-pairs	2
CW pole-pairs	4
Natural speed	500 rpm
Stator slots	48
Rotor slots	36
PW rated voltage	240 V (at 50 Hz)
CW rated voltage	240 V (at 50 Hz)
PW rated current	7 A
CW rated current	7 A
Rated generating torque	100 Nm
Lsp	0.3498 H
Lsc	0.3637 H
Lspr	0.0031 H
Lscr	0.0022 H
Lr	4.4521×10-5H
Rsp	2.3 Ω
Rsc	4 Ω
Rr	1.2967×10-4Ω
J	0.53 kgm2
B	0.036 Nms
Rotor design	Nested-loop
Rated generating torque	100 Nm

Figure 1 illustrates the current tracking in the d-q coordinates using the SMC, ADSMC, and PID controllers. As observed, all three controllers successfully track the desired current; however, the proposed and first order SMCs exhibit lower overshoots compared to the PID controller, while chattering effects are evident in the conventional SMC.
Figures 2 and 3 show powers tracking with the first order SMC, proposed method, and PID controller. After the voltage dip is resolved and the control system is activated, the proposed and first order SMC exhibit lower overshoot compared to the PID controller.

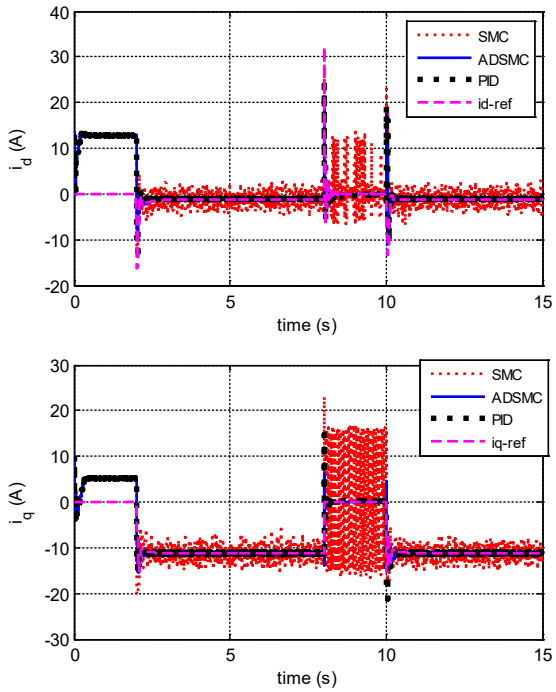

Fig. 2. Current tracking in d-q coordinates by applying SMC, ADSMC and PID methods

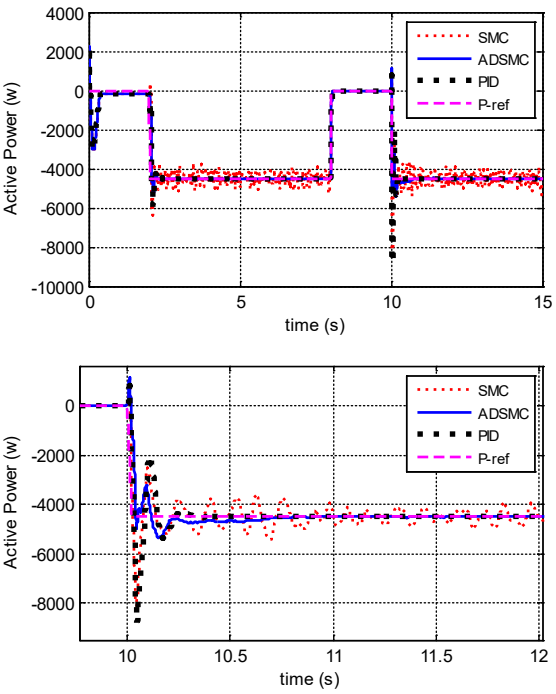

Fig. 3. Tracking active power by applying controllers

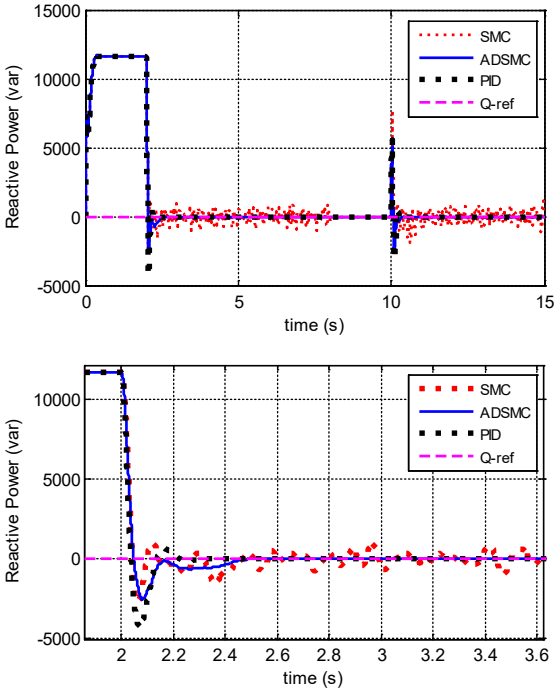

Fig. 4. Tracking the reactive power by applying controllers

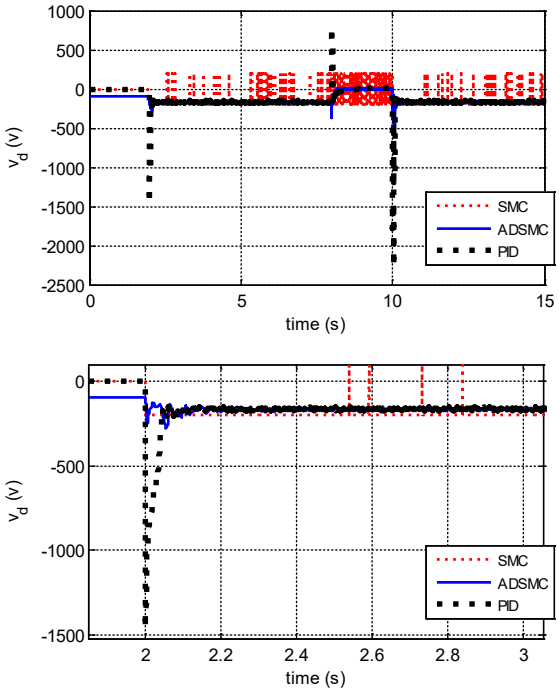

Fig. 5. Control signal along the d-axis in d-q coordinates obtained by applying controllers

Figures 4 and 5 show the control signals generated by the SMC, ADSMC, and PID controllers. The standard SMC exhibits significant chattering effects, hindering its practical implementation. Conversely, the ADSMC method generates smooth control signals, while the PID method produces a control signal with potentially damaging amplitudes, requiring signal saturation to prevent system harm.

Additionally, Figure 6 presents the switching term gains for the conventional and adaptive DSMC methods. Finally, the shaft speed and torque resulting from the application of first order SMC, proposed method, and PID controller are shown in Figure 7.

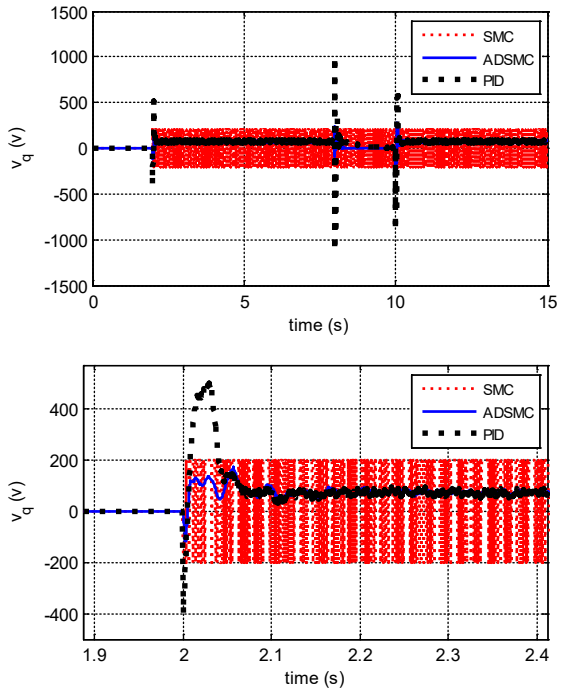

Fig. 6. Control signal along the q-axis in d-q coordinates by controllers

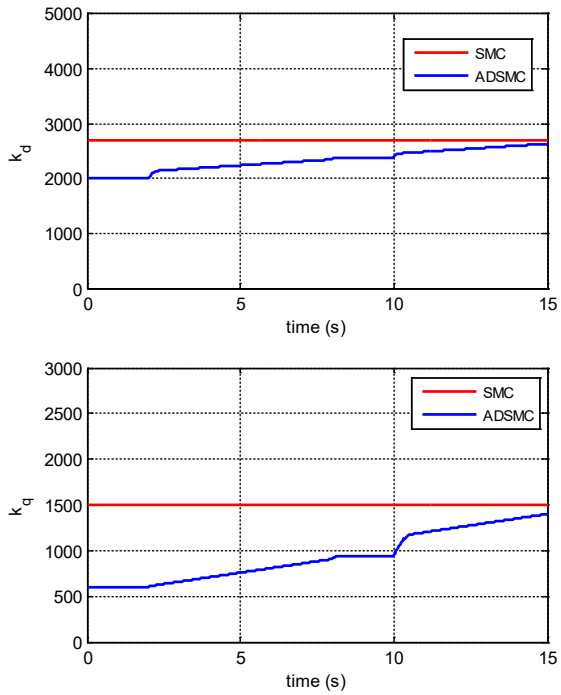

Fig. 7. Switching term gains in first order and the proposed adaptive SMC methods

Now the performance of the proposed method is compared with that of the Second Order SMC (SOSMC). Figure 8 illustrates the current tracking in the d-q directions using the ADSMC and SOSMC controllers. Both controllers accurately tracked the desired current values; however, the ADSMC exhibited lower overshoot compared to the SOSMC. Chattering effects were effectively eliminated in both control methods.

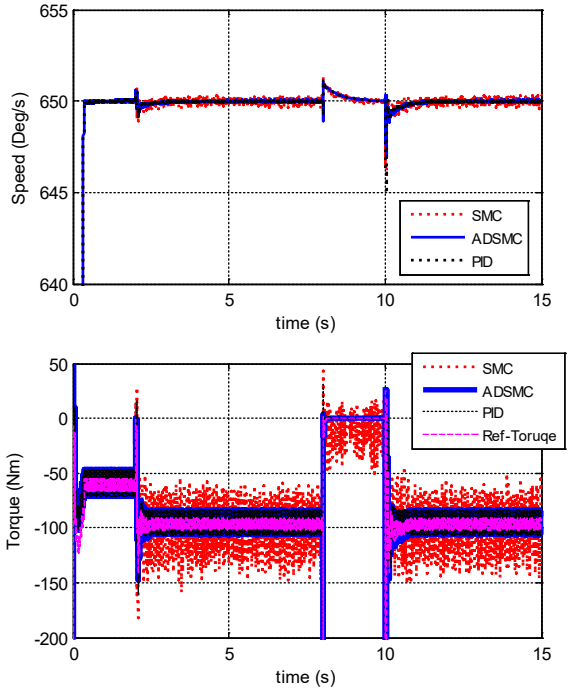

Fig. 8. Shaft speed and torque by applying controllers

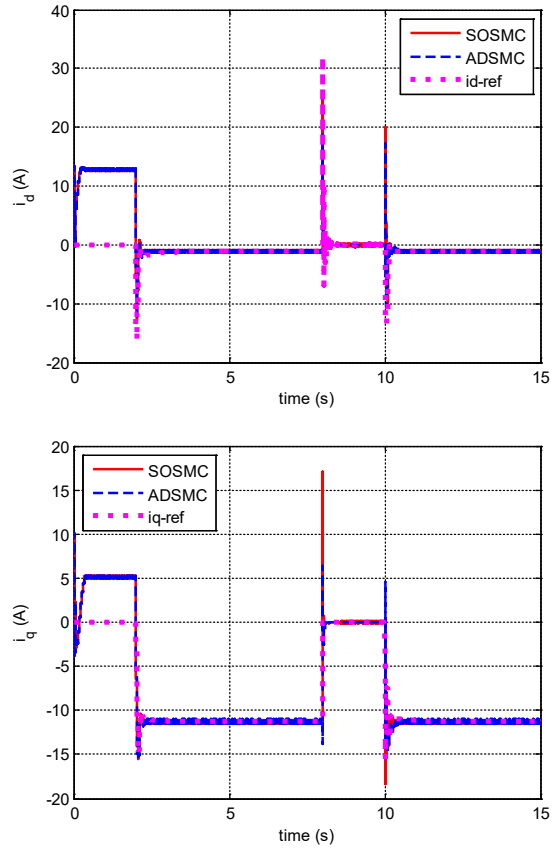

Fig. 9. Current tracking in d-q directions by applying controllers

Figures 9 and 10 illustrate the tracking of powers using the proposed and SOSMC controllers. After the voltage dip is resolved and the controller is activated, the proposed method exhibits fewer overshoots compared to the SOSMC.

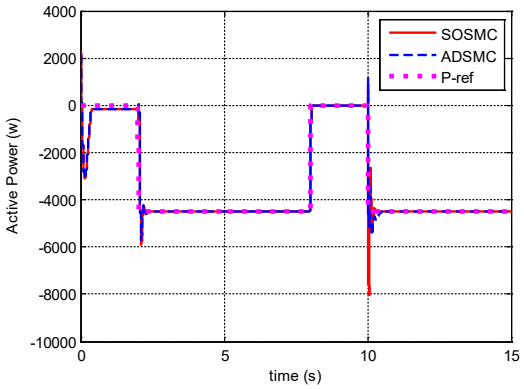

Fig. 10. Tracking the active power by applying controlers

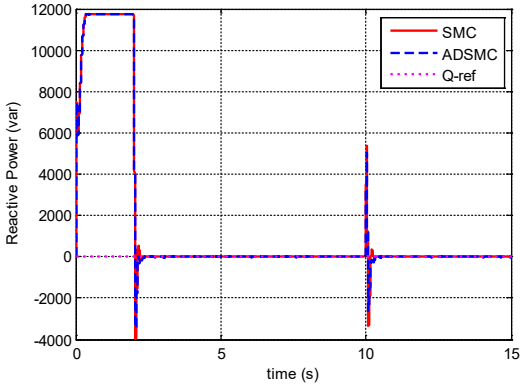

Fig. 11. Tracking the reactive power by applying controllers

Figures 11 and 12 depict the signals generated by the proposed method and SOSMC controllers. Both controllers are free from chattering effects, enabling practical implementation. The signal produced by the proposed method has a lower amplitude compared to that of the SOSMC method. Importantly, the proposed method operates without requiring prior knowledge of the uncertainty upper bound.

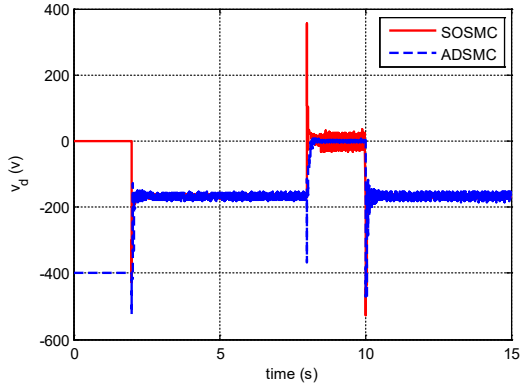

Fig. 12. Control signal along the d-axis in d-q coordinates obtained by applying ADSMC and SOSMC

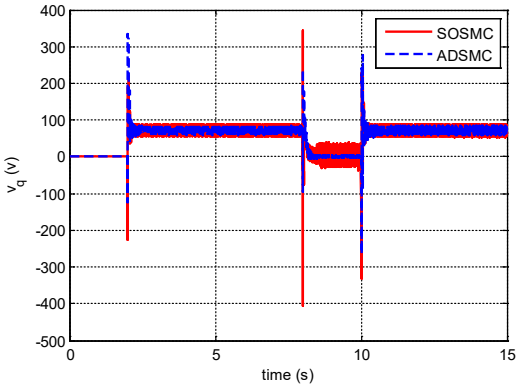

Fig. 13. Control signal along the q-axis in d-q coordinates obtained by applying ADSMC and SOSMC

5 Conclusions

This paper presented an adaptive dynamic sliding mode controller for regulating the powers of BDFIG. The nonlinear control strategy ensures smooth control signals due to its dynamic characteristics, while simplifying implementation compared to conventional sliding mode approaches. By employing adaptive switching gains, the controller eliminates the necessity for prior knowledge of uncertainty bounds, significantly enhancing adaptability and robustness.

Simulations demonstrated that the proposed method delivers smoother signals than conventional SMC, while achieving minimal overshoot compared to PID and second-order SMC methods. Furthermore, the proposed strategy notably reduces the maximum amplitude of the control signal, particularly during system initialization and post-voltage dip recovery, ensuring improved performance under dynamic operating conditions.

Building on these promising outcomes, future research directions include discretizing the control system and conducting hardware-in-the-loop (HIL) testing to validate its practical applicability. Additionally, investigations will explore the integration of model-based and output feedback-based methods, as well as artificial intelligence techniques, to enable real-time adjustment of the switching gains. These steps aim to further enhance the controller's robustness, adaptability, and implementation potential in real-world scenarios.

Disclosure of Potential Conflicts of Interest

The Authors declare that there is no conflict of interest

Reference

[1] O. Moussa, R. Abdessemed, S. Benaggoune, “Super twisting sliding mode control for brushless doubly fed induction generator based on WECS,” International Journal of system assurance engineering and management, Vol. 10, pp. 1145-1157, 2019.

[2] A. Oraee, R. McMahon, E. Abdi, S. Abdi and S. Ademi, "Influence of Pole-Pair Combinations on the Characteristics of the Brushless Doubly Fed Induction Generator," in IEEE Transactions on Energy Conversion, Vol. 35, No. 3, pp. 1151-1159, Sept. 2020, doi: 10.1109/TEC.2020.2982515.

[3] X. Yan and M. Cheng, "A Robustness-Improved Control Method Based on ST-SMC for Cascaded Brushless Doubly Fed Induction Generator," in IEEE Transactions on Industrial Electronics, Vol. 68, No. 8, pp. 7061-7071, Aug. 2021, doi: 10.1109/TIE.2020.3007087.

[4] Ehsani, M. and Oraee, A., 2022. Design of control system based on adaptive sliding mode theory for power tracking in a brushless doubly-fed wind turbine. Journal of Novel Researches on Electrical Power, 10(4), pp.39-47.

[5] X. Yan, M. Cheng, L. Xu and Y. Zeng, "Dual-Objective Control Using an SMC-Based CW Current Controller for Cascaded Brushless Doubly Fed Induction Generator," IEEE Transactions on Industry Applications, Vol. 56, No. 6, pp. 7109-7120, 2020.

[6] D. Zhang, Y. Chen, J. Su and Y. Kang, "Dual-Mode Control for Brushless Doubly Fed Induction Generation System based on Control-Winding-Current Orientation," IEEE Journal of Emerging and Selected Topics in Power Electronics, doi: 10.1109/JESTPE, 2019.

[7] D. Tchioffo, A., Kenmoe Fankem, E.D., Golam, G. et al. "Control of a BDFIG Based on Current and Sliding Mode Predictive Approaches," J Control Autom Electr Syst, Vol. 31, pp. 636–647, 2020.

[8] P. Li, L. Xiong, F. Wu, M. Ma, J. Wang, "sliding mode controller based on feedback linearization for damping of sub synchronous control interaction in DFIG based wind power plants," International journal of electrical power & energy system, Vol. 107, pp. 239-250, 2019.

[9] V. Ghaffari, "A Novel Approach to Designing of Chattering-Free Sliding-Mode Control in Second-Order Discrete-Time Systems," *Iranian Journal of Electrical and Electronic Engineering*, Vol. 15, No. 4, pp. 453-461, 2019.

[10] M. Mbukani and N. Gule, "Comparison of high-order and second-order sliding mode observer based estimators for speed sensorless control of rotor-tied DFIG systems," IET Power Electronics, Vol. 12, No. 12, pp. 3231 – 3241, 2019.

[11] X. Yan and M. Cheng, "A Robustness—Improved Control Method Based on ST-SMC for Cascaded Brushless Doubly Fed Induction Generator," IEEE Transactions on Industrial Electronics, doi: 10.1109/TIE.2020.3007087, 2020.

[12] J. Fei and Y. Chen, "Dynamic Terminal Sliding-Mode Control for Single-Phase Active Power Filter Using New Feedback Recurrent Neural Network," IEEE Transactions on Power Electronics, Vol. 35, No. 9, pp. 9904-9922, 2020.

[13] Ehsani, M., et al. "Adaptive Dynamic Sliding Mode Algorithm for BDFIG Control." Iranian Journal of Electrical & Electronic Engineering 19.1 (2023).

[14] M. Shokoohinia, M. Fateh, & r. Gholipour, "Design of an adaptive dynamic sliding mode control approach for robotic systems via uncertainty estimators with exponential convergence rate," SN Appl. Sci, Vol. 180, No. 2, 2020.

[15] M. Herrera, O. Camacho, H. Smith, "An approach of dynamic sliding mode control for chemical processes," Journal of Process Control, Vol. 85, pp. 112-120, 2020.

[16] Y. Chen and J. Fei, "Dynamic Sliding Mode Control of Active Power Filter With Integral Switching Gain," IEEE Access, Vol. 7, pp. 21635-21644, 2019.

[17] A. Karami and A. Mollaee, H. Tirandaz, O. Barambones, "On dynamic sliding mode control of nonlinear fractional-order systems using sliding observer," Nonlinear Dynamics, Vol. 92, 2018.

[18] R. Hu, H. Deng and Y. Zhang, "Novel Dynamic-Sliding-Mode-Manifold-Based Continuous Fractional-Order Nonsingular Terminal Sliding Mode Control for a Class of Second-Order Nonlinear Systems," IEEE Access, Vol. 8, pp. 19820-19829, 2020.

[19] J. Wang, W. Luo, J. Liu and L. Wu, "Adaptive Type-2 FNN-Based Dynamic Sliding Mode Control of DC-DC Boost Converters," IEEE Transactions on Systems, Man, and Cybernetics: Systems, doi: 10.1109/TSMC.2019.2911721, 2019.

[20] A. Rauf, S. Li, R. Madonski, J.Yang, "Continuous dynamic sliding mode control of converter-fed DC motor system with high order mismatched disturbance compensation," Transactions of the Institute of Measurement and Control, Vol. 42, No. 14, pp. 2812-2821, 2020.

[21] Y. Hu, H. Wang , "Robust tracking control for vehicle electronic throttle using adaptive dynamic sliding mode and extended state observer," Mechanical Systems and Signal Processing, Vol. 135 , 2020,

[22] S. Roy, S. Baldi, L. M. Fridman, "On adaptive sliding mode control without a priori bounded uncertainty," Automatica, Vol. 111, 2020.

[23] Ehsani, M., Oraee, A., Abdi, B., Behnamgol, V. and Hakimi, M., 2024. Adaptive dynamic sliding mode controller based on extended state observer for brushless doubly fed induction generator. International Journal of Dynamics and Control, pp.1-14.

[24] J. Guo, "Application of a novel adaptive sliding mode control method to the load frequency control," European Journal of Control, Vol. 57, 2021.

[25] J. Zhang et al., "Adaptive Sliding Mode-Based Lateral Stability Control of Steer-by-Wire Vehicles With Experimental Validations," IEEE Transactions on Vehicular Technology, Vol. 69, No. 9, pp. 9589-9600, Sept. 2020.

[26] F. Plestan, Y. Shtessel, V. Brégeault, A. Poznyak, "New methodologies for adaptive sliding mode control", International Journal of Control, Vol. 83, No. 9, 2010.

[27] S. Shao, "Control of brushless doubly-fed (induction) machines," Ph.D. dissertation, Dept. Eng., Univ. Cambridge, Cambridge, U.K., 2010.

[28] V. Behnamgol, A. R. Vali, "Terminal sliding mode control for nonlinear systems with both matched and unmatched uncertainties," Iranian Journal of Electrical & Electronic Engineering, Vol. 11, No. 2, 2015.

[29] V. Behnamgol, A. R. Vali, A. Mohammadi and A. Oraee, "Lyapunov-based Adaptive Smooth Second order Sliding Mode Guidance Law with Proving Finite Time Stability," Journal of Space Science and Technology, Vol. 11, No. 2, 2018.